Simultaneous Analysis of Dynamic Crack Growth and Contact of Crack Faces in Single-Region Boundary Element Method

[1]B. Omidvar, [2]M. Rahimian and [2]A. A. DorMohammadi

[1]Natural Disaster Engineering Department,
Graduate faculty of Environment, University of Tehran, P.O. Box: 14155-6135, Tehran, Iran
[2]Department of Civil Engineering, Faculty of Engineering, University of Tehran, Iran

Abstract: In this paper, the formulation of simultaneous analysis of dynamic crack growth and contact of its faces in two-dimensional domain is introduced. Displacement and traction boundary integral equations and additional contact equations are used simultaneously in one region in the time domain. The proposed method has the capability of automatic modeling of crack propagation and contact of crack faces in mixed mode fractures by adding only new elements in front of crack tips. This automatic capability of simultaneous analysis of dynamic discrete crack propagation and contact problem is not enhanced in any of available commercial softwares. In order to verify the proposed method and so as to show the versatile features and capabilities of the method, dynamic crack growth of edge cracks and contact of crack faces in a T shaped plate is analyzed.

Key words: Dual boundary element method . Time domain . Discrete crack propagation . Dynamic fracture mechanics . Contact problem

INTRUDUCTION

Numerical modeling of dynamic crack growth and contact of crack faces has been the subject of intensive research particularly in the last two decades and the results are well documented in the literature. Different methods have been applied by authors to model the dynamic discrete crack growth. Among these models, Finite Element Method (FEM) and Boundary Element Method (BEM) are more applicable. The dynamic fracture mechanics studies cases which inertial effect must be taken into account. These conditions are obtained in dynamic loading or in rapidly growing cracks for static loading.

Discrete crack model in finite element method is shown as separation between element faces. The crack growth along the interface is determined by using fracture mechanics criterion. Crack propagation is determined due to remeshing, creating, replacing or releasing the nodes in finite element model. The main deficiency of this method is high volume of calculation because of repetitious remeshing in analysis or making the primary assumption of crack growth path before analysis. Among the papers dedicated to numerical methods based on discrete crack model in dynamic finite element, one can mention the work of Kobayashi *et al*. [1] and Jung *et al*. [2]. In their works, node release

technique is applied in predicted path for crack growth. In all mentioned works, crack growth path is predicted and assumed before analysis.

In BEM, differential equations are converted into integral equations witch are applied over the boundary. Then the boundary is divided into boundary elements and numerical integration is done over the boundary elements. If boundary conditions are satisfied, as the other numerical methods, a system of linear equations is obtained that can be solved to find the particular solution of the problem.

BEM could be applied for more complex boundary conditions and geometry. In addition, all approximations are carried out over the boundaries in this method. Thus, domains with high gradient variation could be modeled with high accuracy in comparison with FEM. This is the advantage of applying BEM in fracture mechanic problem. BEM requires less time for data preparation due to modeling of boundary and it causes one degree reduction in problem dimension and remeshing. The latter advantage is of so much importance in initial design studies, crack growth and contact problems which need remeshing. Other advantages of BEM are high accuracy in stress and displacement fields in the domain and less memory requirements in comparison with other methods because of reduction of nodes and elements. In

---

Corresponding Author: Dr. B. Omidvar, Natural Disaster Engineering Department, Graduate faculty of Environment, University of Tehran, P.O. Box: 14155-6135, Tehran, Iran

addition, in BEM, inner points are optional, thus the solution can be applied to a certain part of the inner domain.

Reducing the dimension of the problem is one of the positive aspects of BEM. On the other hand, in two-dimensional problems, only the boundary of the region is meshed and in three-dimensional problems only the surface of the region is modeled. In comparison with the other applied methods, BEM leads to a very smaller equation system. In addition, regions with high-stress concentration could be modeled with high efficiency, because in those regions, the dimension of the problem reduces one degree. This is the major reason of applying BEM in fracture mechanic problems.

Dynamic crack growth problem is studied by BEM using different techniques. Gallego and Dominguez [3] applied multi-region BEM in dynamic crack growth problem. They used time-domain with quarter-node elements. In multi-region method, fictitious boundaries which pass through the crack path are not unique. This is the problem of the multi–region method which in step by step analyses of crack growth, fictitious boundaries must be frequently defined at every step of crack growth and this problem makes automatic remeshing a difficult task. Portela *et al*. [4] and MI and Aliabadi [5, 6] presented an application of dual boundary element method (DBEM) for mixed mode crack growth in two-dimensional and three-dimensional linear elastic fracture mechanics. In [7] the time domain method combined with the DBEM presented by Fedelinski for mixed mode rapidly crack growth.

Gonzalez *et al*. [8] have reported an implementation of the DBEM formulation dealing with the analysis of crack growth in structures.

Millings *et al*. [9] have analyzed the dynamic fatigue crack growth by applying the BEM.

Silveira *et al*. [10] have presented a crack growth prediction analysis based on the numerical Green's function and on the minimum strain energy density criterion for crack extension, also known as S-criterion. They have been contemplated crack extensions for two dimensional linear elastic fracture mechanics problems by using BEM.

Lei *et al*. [11] have simulated the dynamic process of propagation and /or kinking of an interface crack in a two dimensional bi-material by applying the multi region BEM.

Yan [12] has developed automated simulation of multiply crack fatigue propagation for two dimensional linear elastic fracture mechanics problems by using BEM. In this paper the displacement discontinuity method with crack–tip element have been proposed by the author.

In the above mentioned references, contact of crack faces is not considered. In this study, the formulation of simultaneous analyses of dynamic crack growth and contact of its faces in time domain is presented. In this formulation, the time domain DBEM is used and the displacement boundary integral equation is applied to one crack surface and the traction boundary integral equation to the other. Also additional contact equations are categorized and applied as constraint equations using static condensation method.

For each increment of crack extension a single region analysis is performed. When the crack propagation is modeled with new discontinuous elements, remeshing of existing boundaries is not required because of the single region analysis application. Further, the new discontinuous elements and the elements on the existing boundaries are employed to construct the total structural mesh representation easily and this is the advantage of the introduced method.

THE TIME DOMAIN DBEM FOR CRACK GROWTH FORMULATION

In non-linear problems, for example when the boundary conditions or geometry of the problem change, superposition principal as in frequency-domain can not be used and the problem must be solved in time-domain. Crack growth in the domain causes non-linearity of the problem and as mentioned before, it should be solved in time-domain.

The displacement integral equation relating the point x' on the boundary Γ of the region V, at time t can be written as [14]:

$$
\begin{aligned}
c_{ij}(x')u_i(x',t) = &\int_\Gamma \int_0^t \left[\begin{array}{c} U_{ij}(x,t;x',\tau)t_i(x,\tau) \\ -T_{ij}(x,t;x',\tau)u_i(x,\tau) \end{array} \right] d\tau d\Gamma(x) \\
&+\rho\int_V \int_0^t \left[U_{ij}(x,t;x',\tau)b_i(x) \right] d\tau dV(x) \quad (1) \\
&+\rho\int_V \left[\begin{array}{c} \dfrac{\partial u(x,0)}{\partial t} U_{ij}(x,t;\zeta,0) \\ +u_i(x,0)\dfrac{\partial U_{ij}(x,t;\zeta,0)}{\partial t} \end{array} \right] dV(x)
\end{aligned}
$$

where u_l is the displacement on the boundary, t_i is the boundary stress vector and ρ is the mass density. The term c_{ij} is jump term which is equal to δ_{ij} when x' is in the domain V and 0.5 δ_{ij} when x' is on the smooth boundary Γ. $U_{ij}(x,t,x',\tau)$ and $T_{ij}(x,t,x',\tau)$ represent the traction and displacement fundamental solutions at a boundary point x at time t due to a unit load placed at location x′ at time τ.

For a problem which is not subjected to body forces and which has zero initial displacement and velocities, the displacement of a point x' can be presented by the following integral equation:

$$c_{ij}(x')u_i(x',t) = \int_\Gamma \int_0^t \left[U_{ij}(x,t;x',\tau) t_i(x,\tau) \right] d\tau d\Gamma(x) - \int_\Gamma \int_0^t \left[T_{ij}(x,t;x',\tau) u_i(x,\tau) \right] d\tau d\Gamma(x) \qquad (2)$$

The mathematical degeneration of the equation (2) when the two crack surfaces are considered coplanar was shown by Kobayashi *et al.* [1]. The symmetric crack geometry problems can be solved by applying symmetric boundary condition and modeling only one of the crack surfaces.

The most general method for crack problem modeling (whether symmetric or not) is dual boundary element method (DBEM). The DBEM incorporates two independent boundary integral equations, which are the displacement equation applied on one of the crack surfaces and the traction equation on the other.

The traction integral equation is obtained by differentiating the displacement equation, applying Hook's low and multiplying by the outward normal at the collocation point. For points which belong to the smooth crack surfaces, the traction equation is:

$$\frac{1}{2} t_j(x',t) = -n_i(x') \int_\Gamma \int_0^t \left[T_{kij}(x,t;x',\tau) u_k(x,\tau) d\tau \right] d\Gamma(x) + n_i(x') \int_\Gamma \int_0^t \left[U_{kij}(x,t;x',\tau) t_k(x,\tau) d\tau \right] d\Gamma(x) \qquad (3)$$

where $n_i(x')$ are components of the outward unit normal vector at the collection point x:U_{kij} $(x,t;x',\tau)$ and T_{kij} $(x,t;x',\tau)$ are fundamental solution of elastodynamics for the traction equation. T_{ij} and U_{kij} and T_{kij} could be obtained by using place differential of U_{ij} [16]:

$$T_{ij} = \lambda \left(\frac{\partial U_{mj}}{\partial x_m} \right) n_i(x) + \mu \left(\frac{\partial U_{ij}}{\partial x_k} + \frac{\partial U_{kj}}{\partial x_i} \right) n_k(x) \qquad (4)$$

$$U_{kij} = \lambda \delta_{ij} \frac{\partial U_{km}}{\partial x'_m} + \mu \left(\frac{\partial U_{kj}}{\partial x'_i} + \frac{\partial U_{ki}}{\partial x'_j} \right) \qquad (5)$$

$$T_{kij} = \lambda \delta_{ij} \frac{\partial T_{km}}{\partial x'_m} + \mu \left(\frac{\partial T_{kj}}{\partial x'_i} + \frac{\partial T_{ki}}{\partial x'_j} \right) \qquad (6)$$

Where λ and μ are the Lame constants.

For numerical solution of a general mixed-mode crack problem, both space and time variations must be discretized. The boundary Γ is divided into M boundary elements in which there are P nodes. The observation time t is divided into N time step sized Q. The time variation of boundary variable is characterized by time step discretization. Displacement and traction are approximated within each element using space interpolation function $N^p(\zeta)$ and within each time step using temporal interpolation function $M^q(\zeta)$. The boundary integral equations are applied for all of the nodes of the boundary elements. The incremental extension of the crack is modeled by adding new elements at its front. The number of the elements in time step n is:

$$M(n) = M_0 + M_c(n) \qquad (7)$$

where M_o is the number of first elements and $M_c(n)$ is the number of added elements which is created because of extension of the crack till step n. After discretizing both space and time variable, the displacement and traction integral equations are [4, 16]:

$$c_{ij}^l u_i^{ln} = \sum_{m=1}^M \sum_{p=1}^P \sum_{n=1}^N \sum_{q=1}^Q \left\{ \begin{array}{l} t_i^{mpnq} \int_{-1}^1 \left[\int_{\tau^{n-1}}^{\tau^n} U_{ij}^{ln}(\zeta,\tau) M^q(\tau) d\tau \right] N^p(\zeta) J^m(\zeta) d\zeta \\ -u_i^{mpnq} \int_{-1}^1 \left[\int_{\tau^{n-1}}^{\tau^n} T_{ij}^{ln}(\zeta,\tau) M^q(\tau) d\tau \right] N^p(\zeta) J^m(\zeta) d\zeta \end{array} \right\} \qquad (8)$$

$$l = 1,2,....,L_1$$

$$\frac{1}{2} t_j^{ln} = n_i^l \sum_{m=1}^M \sum_{p=1}^P \sum_{n=1}^N \sum_{q=1}^Q \left\{ \begin{array}{l} t_k^{mpnq} \int_{-1}^1 \left[\int_{\tau^{n-1}}^{\tau^n} U_{kij}^{ln}(\zeta,\tau) M^q(\tau) d\tau \right] N^p(\zeta) J^m(\zeta) d\zeta \\ -u_k^{mpnq} \int_{-1}^1 \left[\int_{\tau^{n-1}}^{\tau^n} T_{kij}^{ln}(\zeta,\tau) M^q(\tau) d\tau \right] N^p(\zeta) J^m(\zeta) d\zeta \end{array} \right\} \qquad (9)$$

$$l = 1,2,....,L_2$$

where L_1 and L_2 are respectively the number of collection points for which the displacement and the traction equations are applied; $L_1 + L_2 = L$, the total number of nodes; J^m is the Jacobian and ζ is the local coordinate ($-1 \leq \zeta \leq 1$). Note that, in equations (8) and (9), the number of elements and the number of boundary nodes depend on the time observation t, L_1 and L_2 are increased with extension of crack. The place of collection points does not vary with time.

A distinct set of boundary integral equations is obtained by applying the displacement equation (8) for collection points along the external boundary and along one of the crack surfaces and the traction equation (9) for the apposite surface of the crack.

In [16], evaluation of the time integrals and the space integrals has been explained. After discretization, the following matrix equation at the time observation t (stepN) is obtained [16]:

$$[F]^{NN}\{u\}^N = [G]^{NN}\{t\}^N + \sum_{n=1}^{N-1}\left([G]^{Nn}\{t\}^n - [F]^{Nn}\{u\}^n\right) \quad (10)$$

where $\{u\}^N$ and $\{t\}^N$ contain nodal values of displacements and tractions at the time step N; $[F]^{Nn}$ and $[G]^{Nn}$ depend on fundamental solutions and interpolating function. The superscripts Nn emphasize that the matrix depends on the difference between the time steps N and n. The columns of matrices $[F]^{NN}$ and $[G]^{NN}$ are reordered according to the boundary conditions, giving new matrices $[A]^{NN}$ and $[B]^{NN}$. The matrix $[A]^{NN}$ is multiplied by the vector $\{x\}^N$ of unknown displacements and tractions and the matrix $[B]^{NN}$ by the vector $\{y\}^N$ of known boundary conditions, as fallows:

$$[A]^{NN}\{x\}^N = [B]^{NN}\{y\}^N + \sum_{n=1}^{N-1}\left([G]^{Nn}\{t\}^n - [F]^{Nn}\{u\}^n\right) \quad (11)$$

In each time step, only the matrices which correspond to the maximum difference $N - n$ are computed. The rest of the matrices are known from the previous steps. The matrices $[A]^{NN}$ and $[B]^{NN}$ are calculated in the first step only since they are the same at each time step: $[A]^{NN} = A$ and $[B]^{NN} = B$ In order to solve the matrix equation (11), the reverse of $[A]^{NN}$ must be calculated only in the first step. When growing crack, the following phases are considered:

- The direction of crack growth is calculated according to intensity factor and the crack growth speed.
- The new element is added to the front of the growing crack. In this phase the number of nodes is increased.

- For n = 1 matrices $[F]^{NN}$ and $[G]^{NN}$ is calculated according to new geometry of crack.
- For n = 2 to n = N matrices $[F]^{NN}$ and $[G]^{NN}$ have to be corrected. Then matrices $[G]^{NN}$ and $[F]^{NN}$ which have been calculated and the columns and rows which correspond to the new dement and nodes are added and then Matrix $[A]^{NN}$ must be reversed.
- Equation system is solved and the solution process is repeated.

In equation (10), the phrase

$$\sum_{n=1}^{N-1}\left([G]^{Nn}\{t\}^n - [F]^{Nn}\{u\}^n\right)$$

is the effect of loading in previous steps on the current one. When growing crack, note that new nodes which were within the field in previous steps are added to the boundary geometry. It is not required to calculate displacement and traction of these nodes in previous steps.

CONTACT OF CRACK FACES PROBLEM

Contact of crack faces must be considered for more accurate cracked structure behavior simulation. There are three different contact modes

- Stick mode
- Slip mode
- Separation mode

In Fig. 1 a pair of corresponding points on crack faces and their local coordinates is shown. Coulomb's law of limiting friction is considered as a primary principle in study of crack faces. Stick and slip modes are dependent on the coefficient of friction μ. Tangential traction t_t and normal traction t_n in each pair of contact nodes are related to each other as follows:

- $|t_t| < \mu |t_n|$, then contact nodes are stuck together.
- $|t_t| = \mu |t_n|$, then tangential slip between contact nodes is possible. t_t is in the opposite direction of the slip.
- $|t_t| > \mu |t_n|$ is not accepted.

In two dimensional boundary element problems, each node is defined with four variations (t_t, t_n, u_t, u_n). The problem is solved when exactly two of the four variations are known. In contact problems, all four variations are unknown for nodes which are in contact surface. There are eight variations and four equilibrium
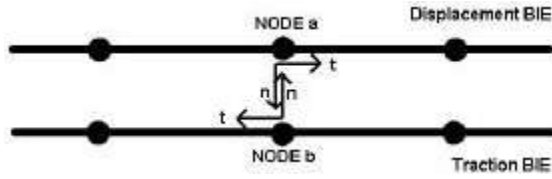
Fig. 1: Two contact elements and two pairs of contact nodes and normal and tangential vector

equations for a pair of contact node and more four equations are added if contact mode is definite.

Additional equations for separation mode can be written as (Fig. 1):

$$\begin{aligned} t_t^a &= 0 \\ t_n^a &= 0 \\ t_t^b &= 0 \\ t_n^b &= 0 \end{aligned} \tag{12}$$

Additional equations for stick mode can be written as (Fig. 1):

$$\begin{aligned} u_t^a + u_t^b &= 0 \\ u_n^a + u_n^b &= 0 \\ t_t^a - t_t^b &= 0 \\ t_n^a - t_n^b &= 0 \end{aligned} \tag{13}$$

Additional equations for slip mode can be written as (Fig. 1):

$$\begin{aligned} t_t^a - t_t^b &= 0 \\ t_n^a - t_n^b &= 0 \\ u_n^a + u_n^b &= 0 \end{aligned} \tag{14}$$

In equation (14), $t_t^a = -\mu t_n^a$ if $t_t^a > 0$ and $t_t^a = +\mu t_n^a$ if $t_t^a < 0$.

Not knowing the contact condition of pair of contact nodes, some iteration are required for satisfying contact conditions in each time step. The algorithm which is applied for preliminary assumption of contact condition of contact nodes and recognition of contact mode is effective on the number of iteration.

In dynamic loading when there are some cracks or a crack in the body, each pair of opposite nodes on crack surfaces can be a pair of contact nodes and there are eight unknown displacement and traction for each pair of contact nodes. Thus after moving the unknown tractions of contact nodes to the other side of the equation, the equilibrium equations of the structure and the additional equations can be written as:

$$\begin{bmatrix} [A]_{n \times n} & [G']_{n \times n} \\ [U]_{m \times n} & [V]_{m \times n} \end{bmatrix} \begin{Bmatrix} \{x\}_n \\ \{t\}_m \end{Bmatrix} = \begin{Bmatrix} \{f^N\}_n \\ \{0\}_m \end{Bmatrix} \tag{15}$$

where n and m are respectively the number of equilibrium equations (twice the number of nodes) and the number of additional contact equations (four times the number of pair of contact nodes); The matrices [U] and [V] are respectively the additional displacement and traction contact equations which have been calculated through equations (12) to (14); {t} contains the traction of the contact nodes. the matrix [A] in equation (15) is the same as the matrix $[A]^{NN}$ in equation (11). {x} is the boundary variable (related to external boundaries) and the displacement variable (related to crack surface nodes). $\{f^N\}_n$ is the time history effects of previous steps in all nodes and effects of loading in current step in external boundary nodes. The matrix [G'] contains the negative values of the $[G]^{NN}$ columns. Each column is related to an unknown member of vector {t}.

The static condensation method is applied for solving the problem in order to save time and memory. The following equations are derived from equation (15):

$$[A]\{x\} + [G']\{t\} = \{f\} \tag{16}$$

$$[U]\{x\} + [V]\{t\} = \{0\} \tag{17}$$

Derived from (16):

$$\{x\} = [A]^{-1}\{f\} - [A]^{-1}\{G'\}\{t\} \tag{18}$$

Substituting {x} from (18) into (17) and calculating unknown in contact nodes {t}, the following is obtained:

$$\{t\} = \left[[U][A]^{-1}[G'] - [V] \right]^{-1} [U][A^{-1}]\{f\} \tag{19}$$

After any iteration, {t} is calculated with the same presumed conditions. If the presumed conditions in all nodes are satisfied, repetition stops. Otherwise the presumed mode is corrected.

Due to the dynamic nature of loading and for achieving numerical convergence, in the first iteration, all the pairs of contact nodes are assumed in separation mode. If in the subsequent iteration, the opposite nodes overlap, they are considered in stick mode. If the real contact mode is slip mode, direction of the tangential traction is easily recognized throughout this approach. Table 1 illustrates the decision state for the mode of contact nodes.

According to Table 1, if contact has happened, Table 2 illustrates the contact mode.
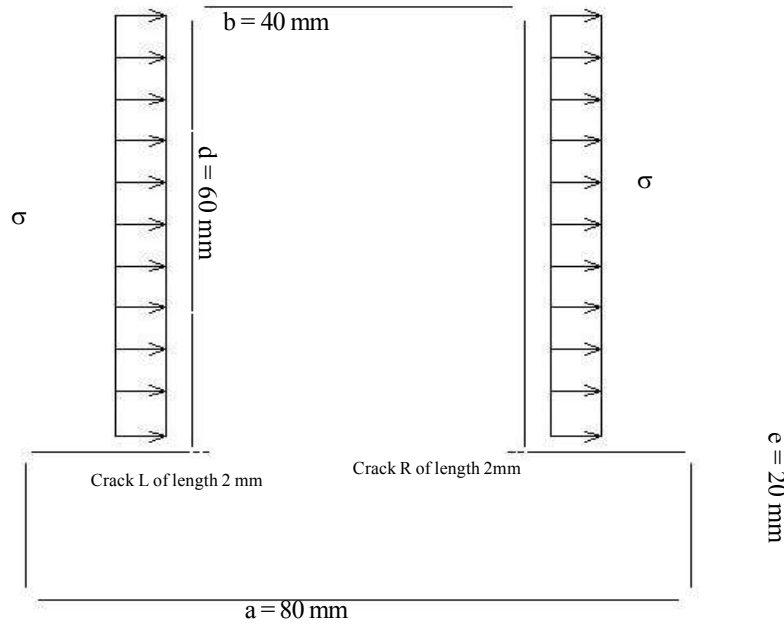
Fig. 2: T-shaped crack with two edge crack under in transverse loading

APPLICATION OF THE PRESENTED METHOD: CRACK GROWTH AND CONTACT OF CRACK FACES IN EDGE-CRACK IN T-SHAPED PLATE:

T-shaped plate has two edge-cracks (Fig. 2). The material properties as below:

Young's modulus $E = 0.2*10^{12}$ pa, Poisson's ratio $\nu = 0.3$, the mass density $\rho = 8000$ kg/m^3. The plate is loaded by the stress σ_0 with Heaviside-function time dependency. The plate is under the state of plane strain. Problem dimensions are:

$a = 80$mm $\quad b = 40$mm $\quad d = 60$mm $\quad e = 20$mm $\quad a_0 = 2$mm

If dynamic stress intensity factor are normalized with respect to K_0($K_0 = \sigma_0\sqrt{\pi a_0}$)

where σ_0 is the applied pressure and a_0 is the initial crack length. The problem is under $\sigma = \sigma_0 H(t)$ loading. Different cases are studied:

Case (a): Crack growth and crack face contacts are not considered. The time step $\Delta T = 1\mu s$ and 300 time steps are considered. The normalized DSIF K_I/K_0 and K_{II}/K_0 are plotted in Fig. 3 the show oscillation around static stress intensity factor this verifies which agree with the results. These factors are as follows:

$$K_{II}/K_0 = 4.71 \qquad K_I/K_0 = \pm 18.02$$

In other words, the above factors oscillate around their corresponding static values which are 18.02 and

Table 1: Illustration of the decision state for the mode of contact nodes

Assumption	Decision	
	--	
Previous	Separation	Contact
Separation	$-u_n^a - u_n^b > 0$	$-u_n^a - u_n^b \leq 0$
Contact	$t_n^a \geq 0$	$t_n^a < 0$

Table 2: Illustration of contact mode

Assumption	Decision	
	--	
Previous	Stick	Slip
Stick	$|t_t^a| < \mu|t_n^a|$	$|t_t^a| \geq \mu|t_n^a|$
Slip	$t_t^a(u_t^a + u_t^b) > 0$	$t_t^a.(u_t^a + u_t^b) < 0$

4.71 in crack L and -18.02 and 4.71 in crack R. Considering the negative value of the normalized DSIF in the first mode in crack R, it is clear that the right side crack must be closed which is simulated later in this paper.

Case (b): Contact of crack faces is considered but crack growth is not. 50 time increments are considered. The normalized DSIF K_I/K_0 and K_{II}/K_0 are plotted in Fig. 4 for the cracks L and R and the equivalent normalized DSIF are also shown. It can be seen that the right side crack R is closed. The nonnegative value of the dynamic stress intensity factor of the mode I of the fracture verifies the formulation of the problem.
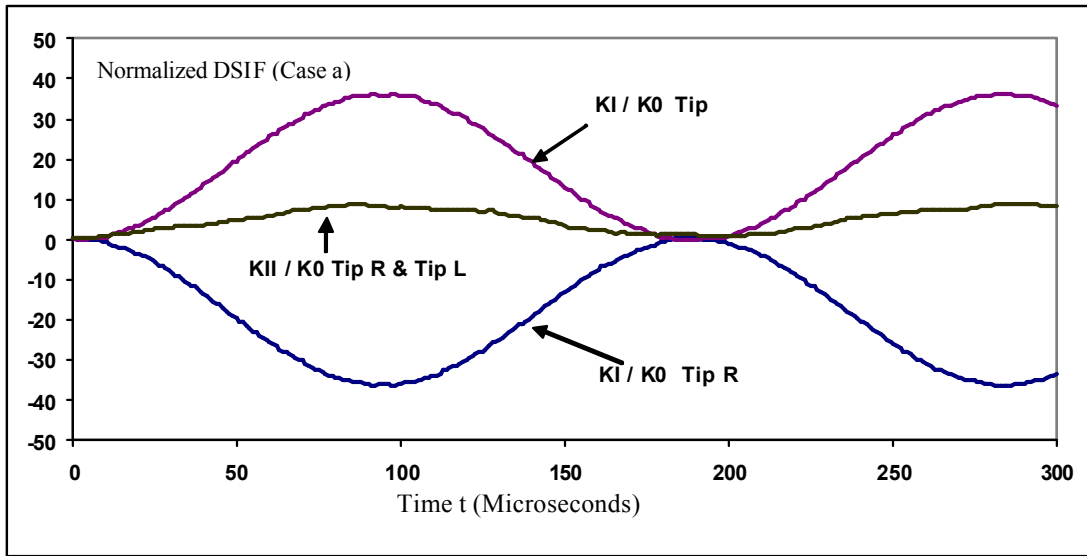
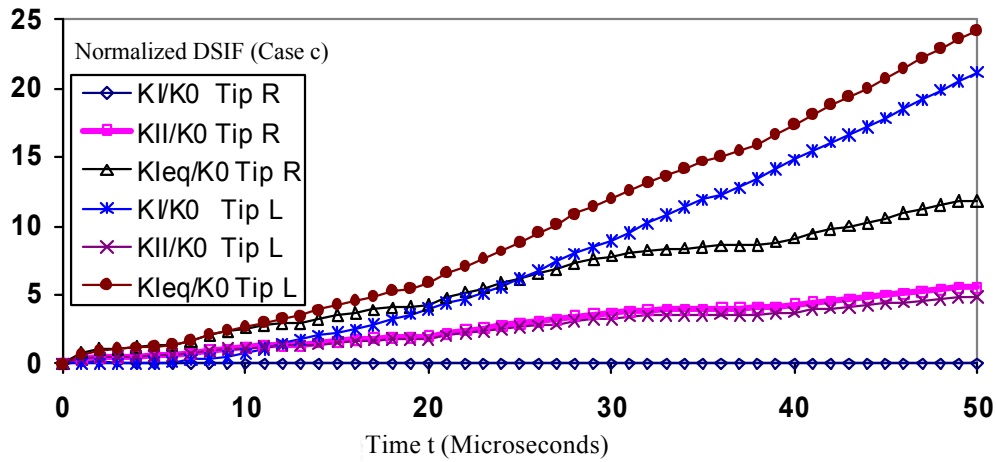Fig. 3: Normalized DSIF for T-shaped plate in transverse loading: Case(a)

Fig. 4: Normalized DSIF for T-shaped plate under transverse loading: Case(b)
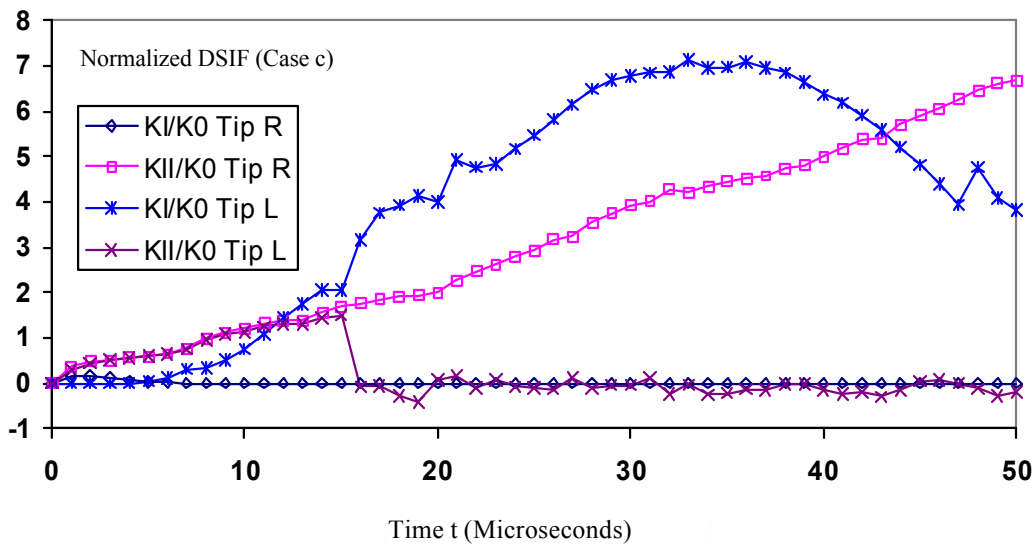

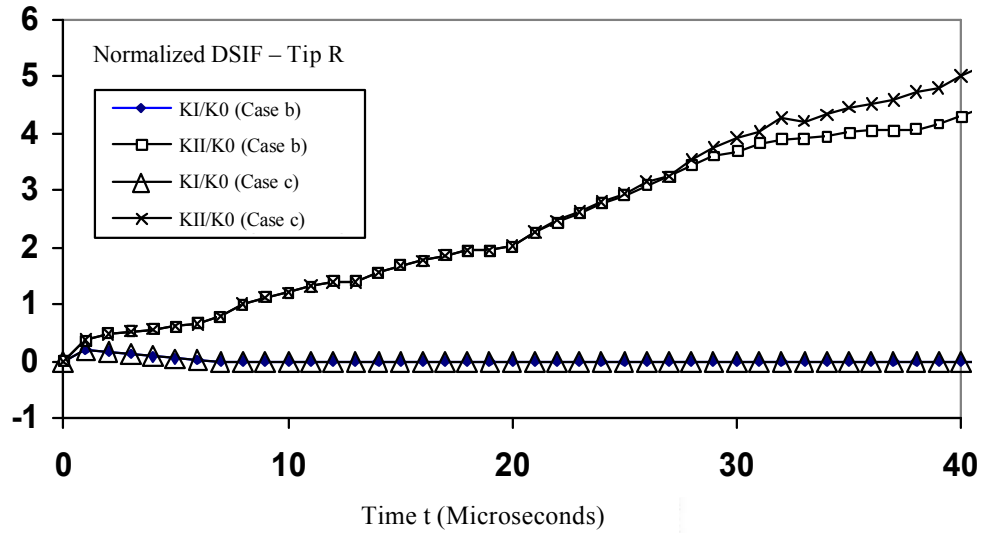Fig. 5: Normalized DSIF for T-shaped plate under transverse loading: Case(c)

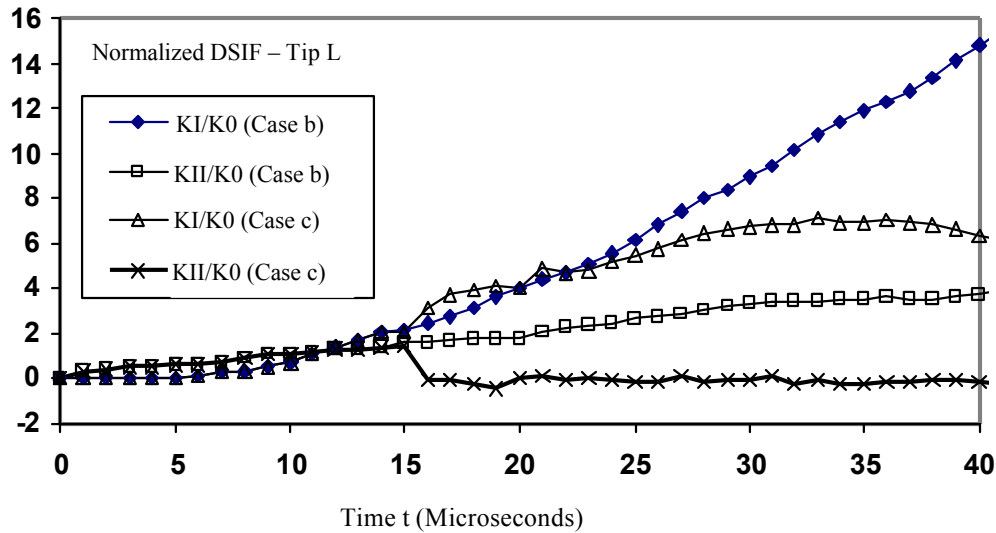Fig. 6: Normalized DSIF for the crack R: Cases (a) and (b)

Fig. 7: Normalized DSIF for the crack L: Cases (a) and (b)

As it can be seen in Fig. 4, by the closing of the crack R, the normalized DSIF in the mode I of the fracture is equal to zero and the mode II DSIF is increased compared to that of crack L. This procedure results in crack L having more tendency for growth compared to crack R. It should be also noted that in this paper, the equivalent dynamic stress intensity factor is equal to the stress intensity factor of the mode I of the fracture which generates the same circumferential stress [16].

Case (c): In addition to considering the contact of the crack faces, the leftmost crack is allowed to grow. For crack L, the normalized critical intensity stress factor for stable cracks is assumed 4. In crack R, the normalized critical intensity stress factor is assumed to

be a large value. The crack growth speed, if needed, is assumed to be 1000 meters per second. [16]

Changes in the normalized stress intensity factors are shown in Fig. 5. It can be seen that the crack growth K_{II} is decreased. In fact, the crack L is grown in a way that the K_I is dominated and the K_2 is considerably decreased. This justifies the change in the crack growth path which is shown in Fig. 5.

The comparison of the normalized stress intensity factors between the cases b and c for cracks R and L is shown in Fig. 6 and 7 respectively.

As it can be seen in Fig. 5-7, crack growth causes stress intensity factor in the second mode of the fracture to decease. The growth of the crack L signifies the slip mode in the crack R. The crack growth path is shown in Fig. 10a.
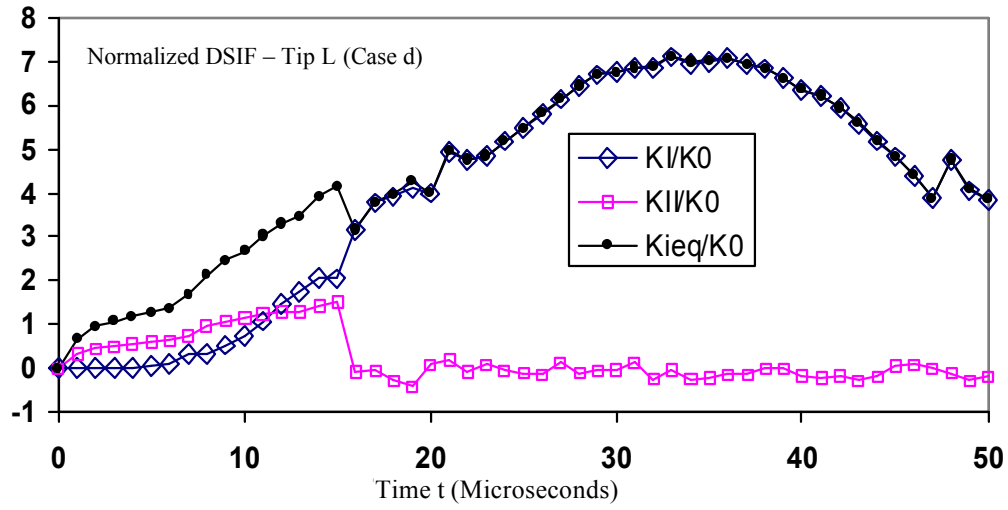
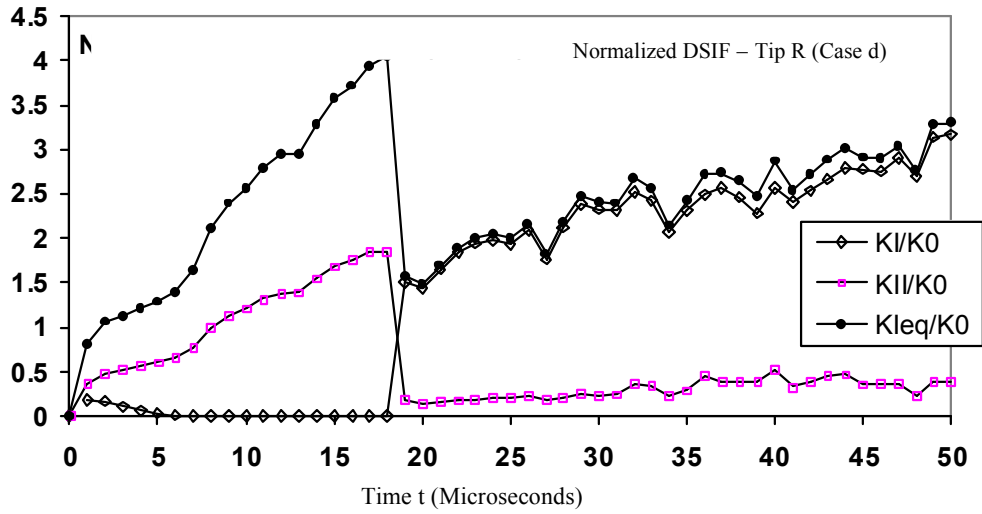Fig. 8: Normalized DSIF for the crack L: Case (d)

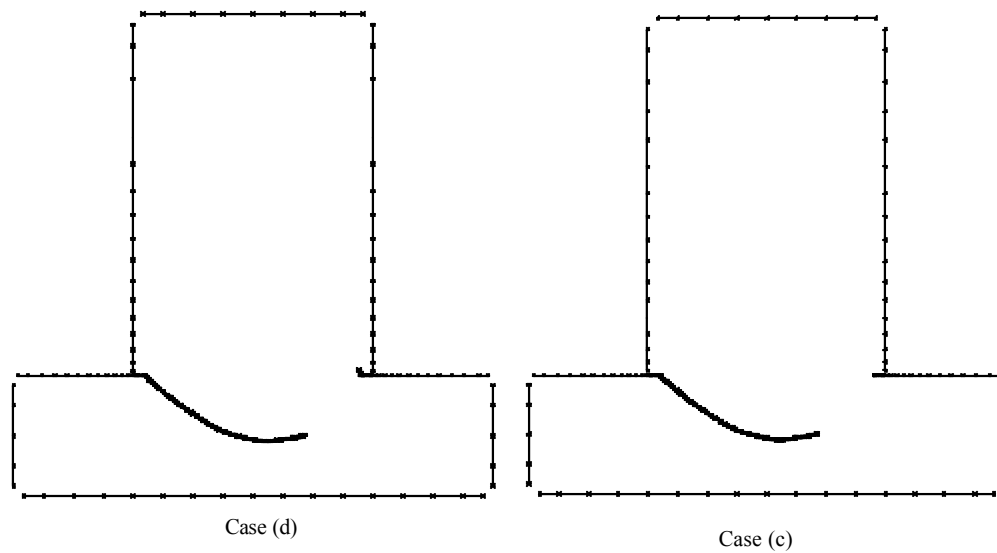

Fig. 9: Normalized DSIF for the crack R: Case(d)

Fig. 10: Crack growth for T-shaped plate in transverse loading: Cases (c) and (d)

Case (d): In addition to the contact of the crack faces, both cracks are allowed to grow. The normalized critical stress intensity factor is assumed 4 for both cracks. The cracks, in case of growth, grow at the speed of 1000 meters per second [16].

Changes in the normalized stress intensity factors in separation mode and slip mode are shown in Fig. 8 and 9.

The growth of the crack L is similar to case (c).Crack R is grown at time step 18 and changes its path which causes K_I to increase and K_{II} to decrease (Fig. 9).The crack growth path is shown in Fig. 10b.

DISCUSSION

One of the difficulties of applying discrete crack model in FEM is the problem of modeling of the crack growth and its path. In other word the crack growth path must be assumed before analysis and remeshing must be done by using compl algorithms while the crack grows. Pre assuming the crack growth path before the analyses leads to notable errors in the results and remeshing algorithm takes so much time especially in dynamic analysis. Note that in singular problems i.e. crack problems and fracture mechanics, results are so dependent on mesh configuration. By applying the presented method, such defects are not faced and the formulation of simultaneous analysis of dynamic crack growth and contact of its faces in the time domain is introduced. In this method, crack is modeled in one region which causes reduction of the analysis time and degrees of freedom. Note that interface cracks can also be modeled with the presented method. With appropriate criterion, crack branching can be analyzed, too. For modeling the grown crack parts, the new elements are added to the crack front and remeshing is not required. The application of this method is shown in growth and contact of edge cracks in T-shaped plates. Free vibration around the static response and the nonnegative values of the mode I stress intensity factor when contact is considered justifies the proposed formulation. It should be noted that in the proposed method, the internal cracks can be modeled with ease. In case of having a proper criteria, the branching of the cracks can be modeled without any additional implementation. In order to model the grown parts, it is enough to add new elements to the tip of the crack without remeshing. The proposed method is applicable in infinite and semi-infinite domains. For instance, fracture and growth of faults growth problems in earthquakes can be solved with this method.

REFERENCES

1. Kobayashi, A.S., A.S. Emery and S. Mall, 1976. Dynamic finite element and dynamic photoelastic analyses of two fracturing Homalite-100 plates. Exper. Mech., 16 (9): 321-328.
2. Jung, J., J. Ahmad, M.F. Kanninen and C.H. Popelar, 1981. Finite element analysis of dynamic crack propagation. Failure prevention and reliability. Proc. of the design engineering technical conference, the design engineer division of ASME, Hartford, Conn.
3. Gallego, R. and J. Dominguez, 1992. Dynamic crack propagation analysis by moving singular boundary element. J. Applied Mech., 59: 158-162.
4. Portela, A., M.H. Aliabadi and D.P. Rooke, 1993. Dual boundary element incremental analysis of crack propagation. Int. J. Comput. Struct., 46: 237-247.
5. Mi, Y. and M.H. Aliabadi, 1994. Three-dimensional crack growth simulation using BEM. Int. J. Comput. Struc., 52: 871-878.
6. Mi, Y. and M.H. Aliabadi, 1995. Automatic procedure for mixed mode crack growth analysis. Commun Numer Methods Eng., 11: 167-177.
7. Fedelinski, D.P., M.H. Aliabadi and D.P. Rooke, 1997. The time-domain DBEM for rapidly growing cracks. Int J. Numer. Methods Eng., 40: 1555-1572.
8. Gonzalez, P., T.F. Pena and F.F. Rivera, 2000. Dual BEM for crack growth analysis on distributed-memory multiprocessors. Advances i Engineering Software, 31: 927.
9. Mellings, S., J. Baynham and R. Adey, 2002. Predicting residual strength using fully automatic crack growth. Engineering Analysis With Boundary Elements, 26: 479-488.
10. Silveira, N.P.P., S. Guimaraes and J.C.F. Telles, 2005. Numerical Green's function for crack growth simulation. Engineering Analysis with Boundary Elements, 29: 978-985.
11. Lei, J., Y.S. Wang and D. Gross, 2007. Two dimensional numerical simulation of crack kinking from an interface under dynamic loading by time domain boundary element method. Int. J. Solids Structures, 6: 10-12.
12. Yan, X., 2007. Automated simulation of fatigue crack propagation for two-dimensional linear elastic fracture mechanic. Problems by boundary element method, Eng Fracture Mechanics, 74: 2225-2246.

13. Cruse, T.A., 1969. Numerical Solution in three dimensional elastostatics. Int. J. Solids Struct., 5: 1259-1274.

14. Brebbia, C.A. and J. Dominguez, 1989. Boundary Elements, An Introductory course. Computational Mechanics Publications, Southampton.

15. Hong, H.K. and J.T. Chen, 1988. Derivation of integral equations of elasticity. Journal of Engineering Mechanics, 114 (6): 1028-1043.

16. Omidvar, B., 2001. The dynamic stability of cracked concrete dams using dual boundary element method in time domain. Ph.D. Thesis, University of Tehran.